colloids and interfaces

MDPI

Article

A Multiple Dynamically Interfacial Cross-Linked PAA/CMCS/QGG Self-Healing Hydrogel for Flexible Wearable Sensing

Qi Wang [1], Chen Xu [1] and Wei Shao [1,2,*]

[1] Jiangsu Co-Innovation Center of Efficient Processing and Utilization of Forest Resources, College of Chemical Engineering, Nanjing Forestry University, Nanjing 210037, China
[2] Jiangsu Provincial Key Lab for the Chemistry and Utilization of Agro-Forest Biomass, Nanjing 210037, China
* Correspondence: w.shao@njfu.edu.cn

Abstract

Traditional single-network hydrogels suffer from unbalanced mechanical and self-healing properties, limited multifunctionality and poor environmental adaptability, severely restricting their applications in flexible wearable sensors. Herein, a multifunctional hydrogel with a semi-interpenetrating network was fabricated via a synergistic multi-crosslinking strategy. The interpenetrating network contains three functional systems: the primary crosslinked network was formed by electrostatic interaction between poly(acrylic acid) (PAA) and cationized guar gum (QGG), a dynamic physical network was constructed by carboxymethyl chitosan (CMCS), and a reinforced reversible crosslinking network was regulated by $AlCl_3$ and naringenin. L-proline was introduced to endow the hydrogel with anti-freezing performance. The reversible imine bonds generated by the Schiff-base reaction between naringenin and carboxymethyl chitosan further enhanced the network dynamic reversibility. The optimized hydrogel exhibited a uniform three-dimensional porous structure that facilitates ion transport and structural deformation. It achieved a tensile strength of 129.3 kPa, a 15 h self-healing efficiency of 98.4%, and reliable adhesion to diverse substrates. With excellent conductivity and sensitive strain sensing capability, the developed hydrogel holds great promise for flexible wearable sensing devices.

Keywords: hydrogel sensor; self-healing; sensitivity

1. Introduction

With the rapid development of wearable electronics and sensing devices, flexible strain sensors that can detect complex human motion and skin deformation have attracted extensive research attention [1–3]. Traditional rigid sensing materials suffer from poor flexibility, low biocompatibility and limited deformation tolerance, which can restrict their practical applications in human motion monitoring and wearable smart devices [4]. Conductive hydrogels with flexibility, mechanical properties and ionic conductivity, have been considered as ideal candidate materials for high-performance flexible strain sensors [5,6].

Nevertheless, conventional single-network conductive hydrogels suffer from unsatisfactory mechanical toughness and stretchability that limit their practical wearable applications. Moreover, the lack of dynamic reversible bonds results in poor self-healing ability and cyclic stability, greatly shortening the service life of wearable sensing devices [7]. To address these issues, the construction of hydrogels with semi-interpenetrating networks (semi-IPN) has

Check for updates

Academic Editor: Elena Mileva

Received: 10 September 2026
Revised: 19 November 2026
Accepted: 20 November 2026
Published: 25 November 2026

Copyright: © 2026 by the authors. Licensee MDPI, Basel, Switzerland. This article is an open access article distributed under the terms and conditions of the Creative Commons Attribution (CC BY) license.

emerged as an effective strategy to optimize the comprehensive performance of hydrogel sensors [8–10].

Poly(acrylic acid) (PAA) is widely used as a typical hydrogel matrix for flexible electronic devices due to its abundant carboxyl functional groups, hydrophilicity and facile formation of dynamic interactions with metal ions [11,12]. For example, a high-performance ionic hydrogel was fabricated from acrylic acid (AA), polyquaternium-10 and $AlCl_3 \cdot 6H_2O$. Taking advantage of the abundant carboxyl groups and hydrophilic nature of the PAA matrix, reversible supramolecular networks were constructed through hydrogen bonding, electrostatic interaction, and Al^{3+} coordination, endowing the hydrogel with greatly improved mechanical robustness, self-healing capability, and reliable ionic conductivity [13]. Another multifunctional conductive PAA-SCMC hydrogel fabricated via the polymerization of sodium carboxymethyl cellulose (SCMC), AA, and alkaline calcium bentonite (AC-Bt) based on hydrogen bond interaction exhibited mechanical performance, high conductivity, favorable self-healing capacity, self-adhesiveness, antimicrobial activity, and 3D printability. It could function as strain sensors, temperature sensors, sweat sensors, and pressure sensors [14]. PAA-polyaniline (PAA-PANI) and polyvinyl alcohol could form IPN backbones through chemical-physical dual crosslinking. The resultant IPN hydrogels achieved high mechanical strength, low swelling, self-healing capability and thermoresponsive shape-memory behavior, showing great promise for self-healing electronics, soft robots and flexible sensors [15].

Natural polysaccharides are promising additives to further tune the performance of PAA-based hydrogels, so rational selection of polysaccharide components is important. Among various polysaccharide candidates, carboxymethyl chitosan (CMCS) was chosen in preference to native chitosan (CS). The introduced carboxymethyl groups endow CMCS with excellent water solubility, which overcomes the poor aqueous solubility of pristine CS [16]. CMCS contains abundant carboxyl and amino groups, which can participate in hydrogen bonding, electrostatic interactions and Schiff base reactions [17,18]. For complementary electrostatic interaction, cationic guar gum hydroxypropyltrimethylammonium chloride (QGG) was further introduced [19]. QGG carries quaternary ammonium groups, which form electrostatic attraction with the negatively charged carboxyl groups of CMCS and PAA. Together, CMCS and QGG introduce multiple reversible interactions within the semi-IPN, facilitating energy dissipation and network self-recovery.

In this work, a multifunctional PAA/CMCS/QGG hydrogel incorporated with naringenin and Al^{3+} was successfully fabricated by constructing a dynamic dual crosslinking network. Compared with many reported PAA-based hydrogels that use only one polysaccharide and possess limited dynamic interactions, two polysaccharides, CMCS and QGG, are paired here to provide distinct electrostatic interactions. Naringenin was introduced to participate in network construction through Schiff base reactions. Benefiting from the combined effect of hydrogen bonds, electrostatic interactions, Schiff base linkages and metal coordination bonds, the prepared hydrogel formed a three-dimensional porous microstructure, which not only provides efficient ion transport channels, but also achieves effective energy dissipation during deformation. Therefore, the hydrogel is expected to present good mechanical toughness and stretchability. The abundant reversible dynamic crosslinks enable the hydrogel with structural recoverability and a high self-healing efficiency, improving the long-term service performance of the hydrogel. Combined with good environmental adaptability and excellent comprehensive performance, the prepared multifunctional hydrogel presents broad application prospects in advanced wearable strain sensing devices, providing a feasible strategy for the design and preparation of high-performance flexible electronic materials.

2. Materials and Methods

2.1. Preparation

5 mL AA, 0.3 g CMCS, 0.06 g proline, 0.15 g QGG, 5 mg *N*,*N*′-methylenebisacrylamide (MBA), 0.7 g $AlCl_3 \cdot 6H_2O$, and different amounts of naringenin were sequentially added into 14 mL of deionized (DI) water under stirring at 500 r/min for 2 h at room temperature. Then the mixture was stirred in a sealed condition under the stirring speed of 200 rpm at room temperature overnight to obtain a homogeneous pre-polymer solution. The pre-polymer solution was transferred to an ice-water bath and stirred at a constant temperature for 10 min, followed by the addition of 0.2 g of ammonium persulfate (APS) pre-dissolved in 1 mL of DI water under stirring for 1 min and then rapidly injected into a mold. The mold was sealed and heated in a constant-temperature water bath at 55 °C for 3 h to complete polymerization. The PAA/CMCS/QGG conductive self-healing hydrogels were obtained. The names and corresponding components of these hydrogels with different amounts of naringenin are listed in Table 1.

Table 1. Components of PAA/CMCS/QGG hydrogels.

Hydrogels	AA (mL)	CMCS (g)	NAR (g)	$AlCl_3 \cdot 6H_2O$ (g)	MBA (mg)	DI Water (mL)	APS (g)	Proline (g)	QGG (g)
$PAA/CMCS/QGG_1$	5	0.3	0	0.7	5	15	0.2	0.06	0.15
$PAA/CMCS/QGG_2$	5	0.3	0.1	0.7	5	15	0.2	0.06	0.15
$PAA/CMCS/QGG_3$	5	0.3	0.2	0.7	5	15	0.2	0.06	0.15
$PAA/CMCS/QGG_4$	5	0.3	0.3	0.7	5	15	0.2	0.06	0.15
$PAA/CMCS/QGG_5$	5	0.3	0.4	0.7	5	15	0.2	0.06	0.15
$PAA/CMCS/QGG_6$	5	0.3	0.5	0.7	5	15	0.2	0.06	0.15

2.2. Characterizations

Surface morphology of the freeze-dried PAA/CMCS/QGG hydrogel was observed on a HITACHI Regulus 8100 Scanning Electron Microscope (SEM) (Hitachi High-Technologies Corporation, Tokyo, Japan). FTIR spectra were acquired on a Spectrum Two spectrometer (4000–400 cm^{-1}, 4 cm^{-1} resolution) (PerkinElmer, Waltham, MA, USA). XPS was performed with an Al Kα source. Open porosity was measured by solvent immersion. Open porosity was calculated as:

$$\text{Open Porosity} = {}^{(W2-W1)}/_{(r \cdot V)} \times 100\% \quad (1)$$

where *W*1 and *W*2 are the dry mass and saturated mass of the hydrogels, V is the bulk volume of cylindrical sample, *r* is the density of ethanol = 0.789 g/cm^3.

Three parallel samples were tested and an average open porosity was determined to be 66.58%.

2.3. Mechanical Properties Determination

Mechanical measurements of the PAA/CMCS/QGG hydrogels with rectangular strips (10 mm × 20 mm × 2 mm) were performed on an electronic universal testing machine (Lishi (Shanghai) Instruments Co., Ltd., Shanghai, China) with the stretching rate of 80 mm/min at 25 ± 2 °C and 60 ± 5% RH. Cyclic tensile tests were conducted and hydrogels were stretched to preset strain and unloaded at 80 mm/min for cyclic loading–unloading to collect hysteresis curves. Lap shear tests were carried out to evaluate the adhesion performance of the PAA/CMCS/QGG hydrogel. Two identical substrates were fixed on glass plates, and hydrogel strips (25 mm × 10 mm × 2 mm) were sandwiched between the substrates. The assembly was stretched on the electronic universal testing machine at 20 mm/min until detachment occurred. All mechanical tests were performed using

5–8 independent hydrogels. Adhesion strength was calculated by dividing the maximum load by the bonding area.

2.4. Self-Healing Test

The hydrogel was cut into two pieces with a scalpel, and the fractured surfaces were brought into contact. After resting for a predetermined time, the self-healing capacity was assessed. Self-healing performance was evaluated from mechanical and sensing performances. The sensing signals of healed hydrogels were recorded using the LCR meter following the aforementioned procedure and compared with pristine samples. Tensile tests of healed hydrogels were conducted on the electronic universal testing machine. Healing efficiency was calculated as:

$$R_S = \frac{\sigma}{\sigma_0} \times 100\% \quad (2)$$

where σ_0 and σ are the fracture stress of the pristine hydrogel and healed hydrogel, respectively.

2.5. Sensing Performance

Conductivity was tested via a two-electrode setup. Conductivity (σ) was determined by the following equation:

$$\sigma = \mathrm{L}/(\mathrm{R}\cdot\mathrm{S}) \quad (3)$$

where L, S and R are the length, area and resistance of the hydrogel, respectively.

Resistance of the PAA/CMCS/QGG hydrogel was measured using an LCR meter (TH2830, Tonghui, Shenzhen, China). The hydrogel was mounted on different positions of human skin as a strain sensor, with copper wires connecting the hydrogel and the LCR meter. Sensor sensitivity under tensile strain was described by the gauge factor (GF), calculated according to the following equation:

$$\mathrm{GF} = \frac{(R - R_0)/R_0}{\varepsilon} \quad (4)$$

3. Results

3.1. Construction of the Multi-Dynamic Crosslinked Hydrogel Network

The PAA/CMCS/QGG hydrogel is prepared via a one-pot thermal-initiated strategy to construct the network through chemical and physical interactions. Upon adding APS and heating to 55 °C, thermally decomposed APS produces sulfate radicals to trigger the free-radical polymerization of AA. MBA acts as a covalent crosslinker to construct a permanent PAA backbone, providing fundamental structural stability. The two polysaccharides (CMCS and QGG) are incorporated into the PAA matrix to form a semi-IPN.

Apart from the covalent skeleton, multiple reversible crosslinks form during and after polymerization. Naringenin provides carbonyl groups to react with primary amines on CMCS and yield dynamic Schiff base bonds (C=N), facilitating dynamic network rearrangement. In addition, its phenolic hydroxyl groups can coordinate with Al^{3+} dissociated from $AlCl_3$ to form stable dynamic metal-phenolic complexes. Al^{3+} further interacts with carboxylate groups on PAA and CMCS to generate metal-carboxylate coordination bonds, which serve as critical physical crosslinks, enhancing mechanical strength and energy dissipation. Electrostatic attraction between positively charged quaternary ammonium groups of QGG and negatively charged carboxylate groups of PAA and CMCS forms polyelectrolyte complexes, further stabilizing the network. Abundant -OH, -COOH, $-NH_2$ and amide groups throughout the system establish extensive intra- and intermolecular hydrogen bonds. The

cyclic structure of proline can further strengthen the hydrogen-bond network and impart anti-freezing properties to the hydrogel.

In short, the hydrogel exhibits a multiscale network structure composed of a covalent structure interconnected with a dynamic supramolecular network. The synergistic combination of covalent bonds, coordination interactions, electrostatic forces and hydrogen bonds enables the hydrogel to achieve self-healing, anti-freezing, self-adhesive, conductive and sensing performances, as explored in the subsequent investigations.

3.2. Morphology and Structure Characterization

SEM image of the PAA/CMCS/QGG hydrogel (Figure 1) reveals a well-defined, highly porous three-dimensional network with interconnected pores. This structure is closely related to the function of the hydrogel as a strain sensor. The open channels facilitate the diffusion of water and ionic species, which supports the ionic conductivity and ensures a rapid and stable electromechanical response to deformation. In addition, the structure provides an effective energy-dissipation mechanism through reversible bending and recovery of the pore walls under mechanical loading, thereby contributing to the toughness of the hydrogel and allowing it to sustain large strains without fracture. Collectively, these morphological features provide a favorable structural basis for the mechanical resilience and sensing performance.

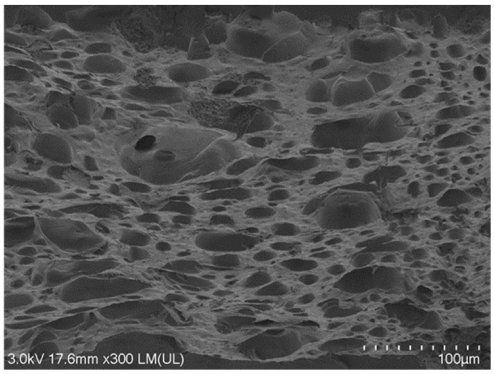


Figure 1. Cross-sectional morphology of PAA/CMCS/QGG hydrogel.

FTIR spectra of the dried hydrogel with and without naringenin (Figure S1). Compared with the control sample, a new absorption peak appearing at 1452 cm^{-1} in the naringenin-containing hydrogel corresponds to the aromatic skeleton vibration of naringenin [20], which confirms the successful incorporation of naringenin into the hydrogel network. For the verification of Schiff base bonds, the peak at 1635 cm^{-1} in the control sample without the addition of naringenin mainly arises from the overlap of carboxylate asymmetric stretching and primary amino N–H bending in the network [21,22]. After the introduction of naringenin, this peak shows a clear increase in intensity at 1635 cm^{-1} originating from the newly formed Schiff base C=N bonds [23], which provides FTIR evidence for the formation of imine structures.

Full survey XPS spectra (Figure S2a) confirm that the Al-free hydrogel contained only C, O and N elements. Clear Al characteristic peaks emerged in the Al-containing sample, verifying the successful introduction of aluminum into the network (Figure S2b). As shown in Figure S2c, a high-resolution Al 2p peak appeared at 74.8 eV, corresponding to trivalent Al species in the hydrogel system. The Al-free hydrogel (Figure S2d) showed a broad O 1s peak at 532.0 eV, due to overlapping signals from different organic oxygen-containing groups. With the addition of Al^{3+}, the O 1s spectrum could be deconvoluted into two components (Figure S2e). The peak at 531.9 eV is assigned to oxygen atoms in coordination bonds and

that at 533.2 eV corresponds to uncoordinated C–O groups. This distinct differentiation of oxygen chemical states provides direct evidence for Al^{3+}-ligand coordination interactions.

3.3. Mechanical Properties

Mechanical flexibility and structural stability are essential properties for hydrogel sensors, enabling them to withstand complex deformations in wearable device applications. Herein, the mechanical performances of the PAA/CMCS/QGG hydrogel were systematically investigated. As shown in Figure 2, the hydrogel exhibited favorable stretchability and could be stretched to a large strain. It resisted various severe deformations such as knotting and twisting without any structural failure. Remarkably, the hydrogel was capable of stably supporting a 200 g weight (430 times its own mass).

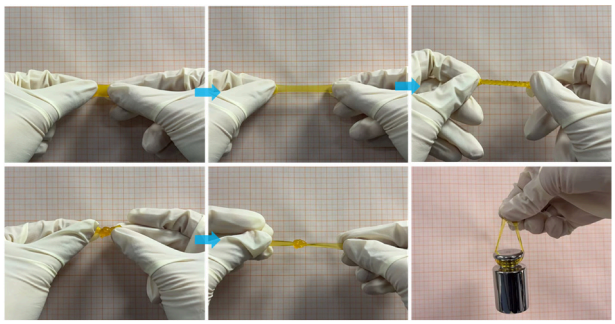


Figure 2. Photographs of PAA/CMCS/QGG hydrogels showing the ability to withstand being stretched, twisted, knotted and lift a 200 g weight.

To further explore the influence of naringenin dosage on the mechanical properties of the PAA/CMCS/QGG hydrogels and determine the optimal formulation, hydrogel samples with gradient naringenin contents were prepared for comparative investigation. Tensile tests were performed on all groups, and the corresponding stress–strain curves are displayed in Figure 3. It can be seen that the tensile strength of the hydrogel gradually increased from 72.8 kPa to 129.3 kPa with the increase in naringenin content from 0 g to 0.3 g (Table S1). Such mechanical improvement originates from the increased crosslinking density induced by metal–phenolic coordination interactions, Schiff base linkages, and abundant hydrogen bonds derived from phenolic hydroxyl groups of naringenin. The increased reversible crosslinks can dynamically break and reconstruct during mechanical deformation, effectively dissipating energy and strengthening the hydrogel network structure [24]. Nevertheless, excessive naringenin could cause a reduction in fracture stress [25]. This phenomenon is ascribed to the over-crosslinked network which greatly limits the movement of polymer chains under stretching. Overall, the hydrogel with 0.3 g naringenin achieved the optimal comprehensive mechanical performance, possessing the maximum fracture stress while retaining desirable stretchability, which balances material strength and flexibility well. Consequently, 0.3 g naringenin was determined as the optimal dosage for subsequent experimental preparation.

The anti-fatigue and self-recovery performance of the hydrogel were investigated using continuous loading–unloading cyclic tensile tests. First, cyclic tensile measurements were performed at different preset maximum strains (100–500%). As displayed in Figure S3a, each cycle exhibited a distinct hysteresis loop, and good overlap was observed between adjacent cyclic curves, which suggests the favorable self-recovery capability and resilience of the hydrogel. The fatigue resistance was further evaluated by 10 successive loading–unloading cycles at a maximum strain of 300%. The first cycle exhibited an evident hysteresis loop (Figure S3b), which corresponds to energy dissipation caused by the rupture of

dynamic noncovalent bonds within the network. The hysteresis area and dissipated energy gradually declined with increasing cycle number and tended to stabilize after several cycles (Figure S3c). A minor residual strain appeared after the first unloading, but showed no noticeable increase in subsequent cycles, suggesting that the network gradually entered a stable reversible deformation state. These observations imply that the hydrogel has desirable self-recovery behavior.

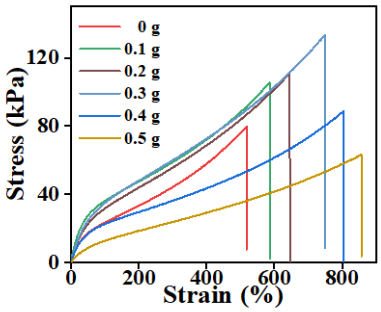


Figure 3. Tensile stress–strain curves of PAA/CMCS/QGG hydrogels with different naringenin dosages.

Apart from mechanical robustness at ambient temperature, the low-temperature resistance of the PAA/CMCS/QGG hydrogel was also evaluated. As displayed in Figure 4, after being stored at −20 °C for 48 h, the hydrogel still maintained flexibility and was capable of undergoing large tensile deformations, which is similar to the hydrogel tested at room temperature, with no structural fracture. A control hydrogel without the introduction of L-proline was fabricated for comparison (Figure S4). After freezing, the L-proline-free hydrogel turned brittle and fractured once bent. The anti-freezing capability is mainly attributed to the introduction of L-proline, which effectively inhibits the formation and growth of ice crystals inside the polymer network [26,27]. Different from conventional hydrogels which easily stiffen and embrittle at low temperatures, the prepared hydrogel maintained stable mechanical flexibility and stretchability under subzero environments, greatly improving the environmental adaptability of wearable hydrogel sensors.

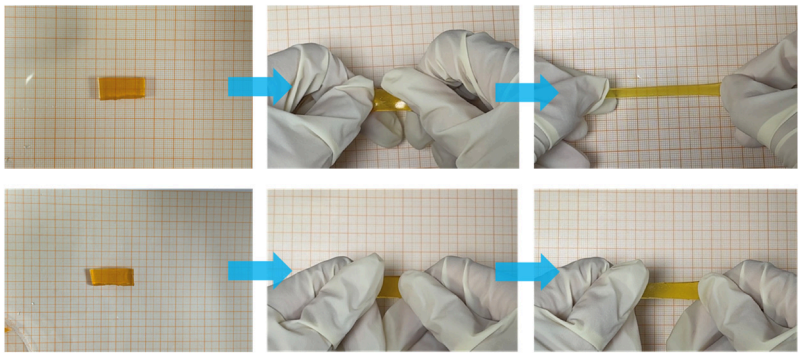


Figure 4. Comparison of tensile behaviors of the hydrogels before and after freezing at −20 °C ((**top**): unfrozen hydrogel; (**bottom**): hydrogel frozen at −20 °C for 48 h). Tensile tests were performed immediately after the frozen samples were removed from −20 °C.

3.4. Self-Adhesive Performance

Self-adhesive capability is an essential performance for high-performance wearable strain sensors, which ensures conformal attachment between the sensor and diverse substrate surfaces to avoid interfacial failure during service. As shown in Figure 5, the hydrogel could tightly adhere to various common substrates, including human skin, paper, wood, copper foil, aluminum foil and plastic, without additional adhesive aids, demonstrating

good self-adhesion performance. The adhesive behavior originates from the abundant polar functional groups distributed throughout the hydrogel, including carboxyl groups, hydroxyl groups, naringenin-derived phenolic hydroxyl groups, and quaternary ammonium groups. These active groups can synergistically generate multiple interfacial non-covalent interactions, such as hydrogen bonding, electrostatic attraction, hydrophobic association, and metal-ligand coordination, endowing the hydrogel with good interfacial binding force [28,29]. Such self-adhesion is highly desirable for wearable sensing applications, which guarantees stable signal transduction, which is crucial for the reliable sensing performance of wearable strain sensors.

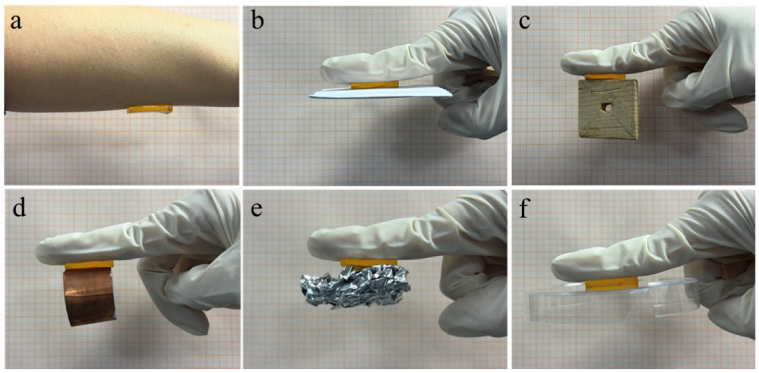


Figure 5. The photographs of the hydrogel adhered to human skin (**a**), paper (**b**), wood (**c**), copper foil (**d**), aluminum foil (**e**) and plastic (**f**).

3.5. Self-Healing Performance

Self-healing performance is an essential property of wearable hydrogel sensors, which can self-repair structural damage caused by repeated mechanical deformation, effectively prolonging the service life of the devices [30]. The self-healing behavior of the PAA/CMCS/QGG hydrogel was first verified through macroscopic qualitative experiments. Firstly, hydrogels with different shapes were prepared for self-healing tests. Hydrogels were cut into two separate parts, with one part stained with methyl orange to achieve clear color distinction. The fresh-cut interfaces of different-colored hydrogels were closely contacted and placed at room temperature for 15 h. As displayed in Figure 6a, the healed hydrogel could be stretched without interfacial fracture, demonstrating the good macroscopic self-healing capability of the hydrogel.

Tensile tests were further carried out to quantitatively assess the mechanical recovery performance of the hydrogel after healing. The stress–strain curves of hydrogels with different healing times are shown in Figure 6b. After 15 h of room-temperature healing, the self-healing efficiency of the pristine control hydrogel without naringenin was calculated to be 31.08% (Figure S5). After the introduction of naringenin into the hydrogel, the self-healing efficiency of the hydrogel reached as high as 98.4% (Figure 6c), indicating great self-healing ability. The self-healing performance originates from the reversible dynamic bonds, including hydrogen bonds, electrostatic interactions, Schiff base linkages, and Al^{3+}-mediated metal–phenolic coordination bonds, without destroying the overall network structure [31,32]. When the fractured interfaces are closely contacted, these dynamic bonds can spontaneously reconstruct at the contact interface. In addition, the flexible and mobile polymer chains further facilitate the reconnection of the fractured network. The high self-healing behavior endows the hydrogel with excellent mechanical durability and damage tolerance, which guarantees its long-term stable service in wearable sensing devices.

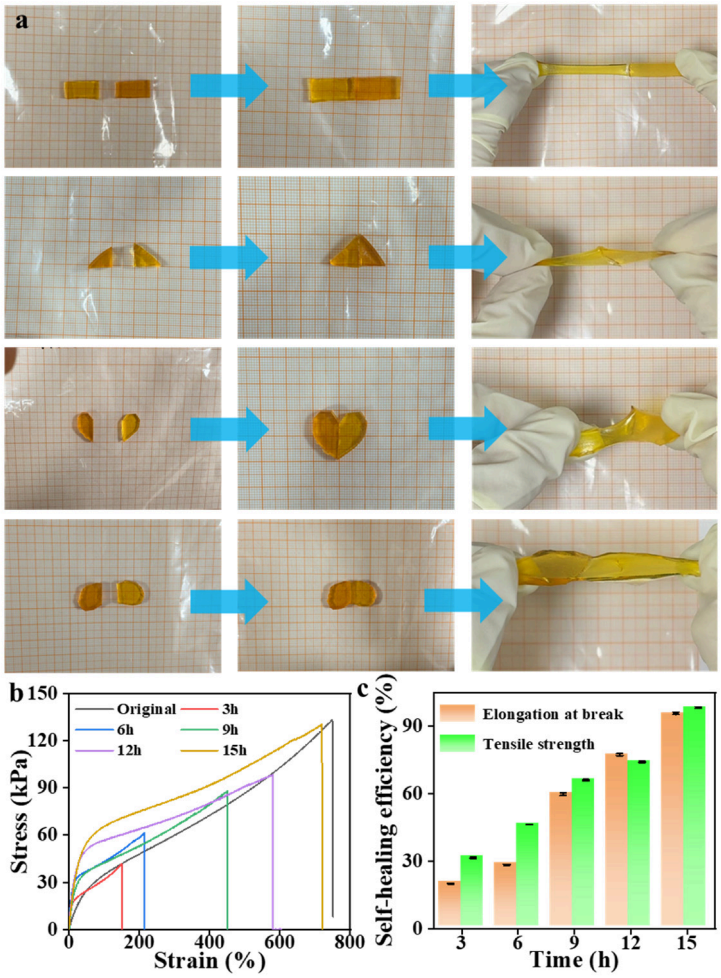


Figure 6. (**a**) Photos of self-healing performance of PAA/CMCS/QGG hydrogels and their stress–strain curves (**b**) and the healing efficiencies (**c**) after healing for different times.

3.6. Electrical Conductivity and Strain Sensing Performance

The prepared PAA/CMCS/QGG hydrogel exhibited a favorable ionic conductivity of 1.8 S/m (Figure S6). A simple circuit test was further performed to verify its conductive ability (Figure 7). When the hydrogel was connected in series with an LED, the circuit was successfully switched on and the LED lit up, confirming the electrical conductivity of the prepared hydrogel. In addition, the LED brightness gradually weakened as the hydrogel was stretched to larger tensile strains. This visible brightness variation reflects the strain-dependent ionic conduction behavior of the hydrogel. During stretching, the internal conductive pathways are elongated and narrowed, increasing the ion transport distance and reducing the effective transport area. These microstructural changes collectively increase the hydrogel resistance and weaken ionic conduction. Such reliable mechano-electrical responsiveness enables the hydrogel to produce stable electrical signals in response to mechanical deformation, demonstrating its great potential for wearable strain sensing applications.

High sensitivity and stable electrical responsiveness are key requirements for high-performance wearable strain sensors, which determine the accuracy and reliability of mechanical signal detection. The gauge factor (GF) is a critical index to quantitatively evaluate the sensing sensitivity [33]. The strain-responsive electrical behavior of the PAA/CMCS/QGG hydrogel was quantitatively analyzed, and the corresponding sensing curves are presented in Figure 8a. The relative resistance increased with the increase in applied strain, while the GF value presented a stepwise growth in different strain ranges.

Specifically, the GF value was 3.84 within the strain range of 0–300%, increased to 9.25 at 300–600%, demonstrating high sensing sensitivity across both low and high strain regions over a broad deformation range. Such gradient sensitivity enables the hydrogel to achieve high-precision sensing over a wide deformation range, showing great application prospects in multifunctional wearable sensing devices.

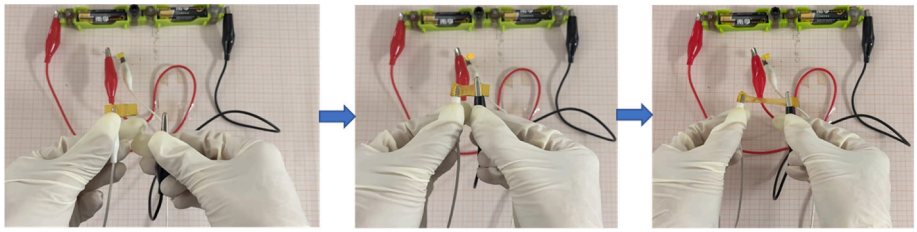


Figure 7. Photographs of LED was lighted by the PAA/CMCS/QGG hydrogel and its brightness changed with the strain of the hydrogel.

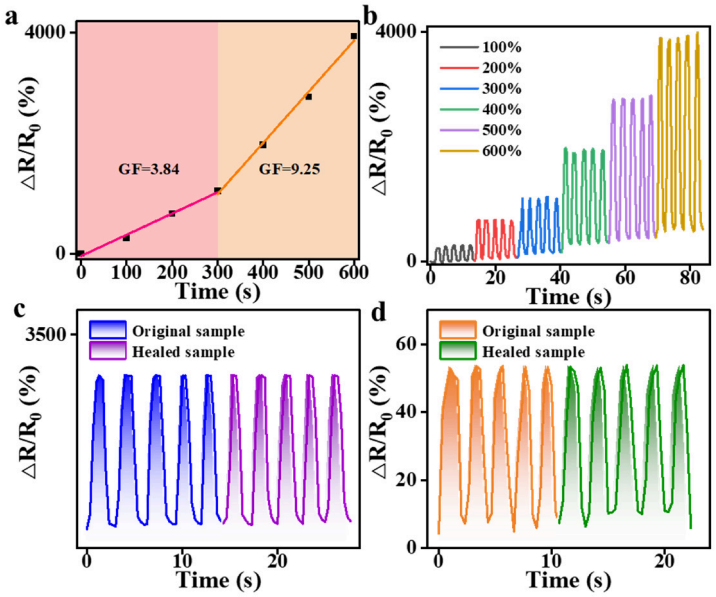


Figure 8. (**a**) GF values of the PAA/CMCS/QGG hydrogel sensor (Pink: strain range of 0–300%, orange: strain range of 300–600%). (**b**) Cyclic relative resistance responses of the hydrogel sensor at progressively increasing strains (100–600%). (**c**) Cyclic resistance changes in the original and healed hydrogel sensors at strains 500%. (**d**) Monitoring of finger bending of the original and healed hydrogel sensors.

Cyclic sensing stability is critical for the long-term service of wearable strain sensors. Stepwise cyclic loading–unloading tests were first conducted across strains of 100% to 600% to evaluate the sensing reversibility over a wide deformation range (Figure 8b). At each strain level, $\Delta R/R_0$ exhibited reproducible periodic responses matching the loading–unloading cycles. The peak $\Delta R/R_0$ increased with increasing strain, and the signal recovered to near the initial baseline upon each unloading, indicating that the sensor maintains reliable and distinguishable sensing responses under different deformations. To further examine the long-term cyclic durability, continuous loading–unloading cycles were performed at a fixed strain of 500% (Figure 8c). The pristine hydrogel sensor delivered regular and highly consistent electrical signals throughout the repeated cycles, verifying good mechano-electrical cycling stability for prolonged wearable operation. The hydrogel after 15 h of self-healing exhibited nearly identical cyclic resistance profiles and signal amplitude to the

pristine sample under the same 500% strain, confirming that the sensing stability is well retained after network reconstruction.

To further verify its practical applicability in human motion monitoring, the hydrogel sensor was attached to a finger joint to detect bending motions (Figure 8d). As the finger flexed, the hydrogel stretched along with the skin, generating a clear rise in relative resistance. When the finger returned to the straight position, the sensing signal quickly recovered to its initial baseline. Under the same test conditions, the healed hydrogel showed nearly identical response patterns and signal amplitude, with no evident degradation in dynamic response or reversibility. A comparison of mechanical properties, self-healing efficiency, conductivity, and GF values between PAA based hydrogels [11,32,34–41] and this work is listed in Table S2. It can be clearly seen that the fabricated hydrogel exhibits good a competitive overall performance. These results confirm that the PAA/CMCS/QGG hydrogel delivers favorable dynamic response and reversible sensing performance both before and after self-healing, making it suitable for reliable long-term wearable motion detection.

4. Conclusions

In this work, a multifunctional PAA/CMCS/QGG hydrogel with a dynamically crosslinked three-dimensional porous network was successfully prepared. The unique interconnected porous microstructure endows the hydrogel with efficient ion transport channels and effective energy-dissipation behavior, which collectively guarantee its favorable ionic conductivity and good mechanical properties. Relying on multiple reversible dynamic interactions, the obtained hydrogel exhibited reliable mechanical flexibility, good low-temperature stability, and great self-healing performance with a high healing efficiency of 98.4%. Notably, the hydrogel delivered excellent strain-sensing performance with high sensitivity over a wide strain range, achieving stable and reversible electrical responses during cyclic deformation and precise monitoring of human joint motion. Combining the mechanical adaptability, high-sensitivity strain responsiveness, and great self-healing ability, the PAA/CMCS/QGG hydrogel shows great potential for advanced wearable strain sensor applications. The leaching behavior of naringenin and L-proline under aqueous or sweat conditions will be carried out in our further study.

Supplementary Materials: The following supporting information can be downloaded at https://www.mdpi.com/article/10.3390/colloids10060091/s1. Figure S1: FTIR spectra; Figure S2: XPS spectra; Figure S3: Tensile loading-unloading curves; Figures S4 and S5: Tensile behaviors; Figure S6: The conductivity values; Table S1: Mechanical properties; Table S2: Comparison of mechanical properties, self-healing efficiency, conductivity, and GF values.

Author Contributions: Conceptualization, Q.W. and W.S.; methodology and data curation, Q.W. and C.X.; writing—original draft preparation and review and editing, W.S. All authors have read and agreed to the published version of the manuscript.

Funding: This research received no external funding.

Data Availability Statement: Data will be made available upon request.

Conflicts of Interest: The authors declare no conflicts of interest.

References

1. Huang, K.; Zhou, J.; Xiao, A.; Lin, B.; Huang, Z.; Wu, T. A versatile hydrogel for sensing-energy storage integrated wearable electronics. *Chem. Eng. J.* **2025**, *526*, 171315. [CrossRef]
2. Jiang, P.; Meng, Q.; Qu, D.; Wu, Z.; Liang, Y.; Zhang, X. Mussel-inspired tannic acid-integrated hydrogel with strong adhesion and anti-freezing stability for wearable sensing. *Polymer* **2026**, *364*, 130696. [CrossRef]

3. Luo, Q.; Xu, Y.; Wu, Z.; Xu, Y.; Yang, Y.; Dai, J.; Jiang, J.; Jia, R.; Liu, H.; Fu, H.; et al. Electrochromic double-network hydrogel for flexible strain sensing and on-board energy storage in wearable devices. *J. Colloid Interf. Sci.* **2026**, *721*, 140749. [CrossRef] [PubMed]
4. Tian, B.; Ye, F.; Ma, H.; Zhao, C.; Lin, Z.; Sun, Q.; Hu, X.; Ang, R. Thermoelectric composite hydrogels with ionic-electronic transport for bioactive energy harvesting and sensing. *Nano Energy* **2026**, *153*, 111940. [CrossRef]
5. Yang, M.; Li, B.; Qiao, L.; Liu, G.; Yin, B.; Guo, M.; Song, H.; Wang, X. Highly stretchable, healable and conductive mxene-based multifunctional hydrogel for flexible strain sensors. *Sens. Actuators A-Phys.* **2026**, *411*, 118431. [CrossRef]
6. Moreno, J.M.C.; Chelu, M.; Popa, M. Eco-friendly conductive hydrogels: Towards green wearable electronics. *Gels* **2025**, *11*, 220. [CrossRef] [PubMed]
7. Lan, Y.; Liu, G.; Li, M.; Liu, C.; Wei, J.; Lin, M.; Chen, X.; Li, Z. Mechanically robust hydrogel wearable sensor with bentonite-reinforced poly(acrylic acid-acrylamide) network. *Sens. Actuators A-Phys.* **2026**, *410*, 118152. [CrossRef]
8. Yang, X.; Li, K.; Luo, H.; Li, J. Dual-functional semi-interpenetrating network hydrogels for synergistic adsorption and selective detection: Experimental investigation coupled with dft calculations. *Sep. Purif. Technol.* **2026**, *405*, 138965. [CrossRef]
9. Guo, C.; Niu, C.; Li, Y.; He, J.; Shi, J.; Wang, Y.; Zhao, K. Regulable preparation of pda-integrated silk fibroin/polyvinyl alcohol composite hydrogels with interpenetrating network for nir-triggered drug release. *Chem. Eng. Sci.* **2026**, *320*, 122662. [CrossRef]
10. Yan, T.; Liang, M.; Yang, S.; Zhang, L.-Z. A semi-interpenetrating network hydrogel electrolytes doped with nanoparticles for highly stable zinc-ion batteries. *J. Power Sources* **2026**, *685*, 240456. [CrossRef]
11. Liu, J.; Cui, Y.; Zhang, R.; Liu, P. Dynamic Fe^{3+} coordination network-enabled cmc-na/paa conductive self-healing hydrogels for flexible strain sensing applications. *Polymer* **2026**, *365*, 130737. [CrossRef]
12. Luo, Y.; Wang, Z.; Zhao, Z.; Zhu, M. Multi-functional performance of injectable ultra-stretchable nickel ion-mediated polyacrylic acid/dmso hydrogels for flexible electronic sensor. *J. Mater. Sci. Technol.* **2026**, *271*, 318–328. [CrossRef]
13. Zou, J.; Yang, Z.; Liang, J.; Xie, Y.; Fan, M.; Zhang, X. Recyclable, high strength and electrical-mechanical self-healing wearable ionic hydrogel sensor. *Polymer* **2024**, *315*, 127826. [CrossRef]
14. Wei, J.; Liu, C.; Shi, L.; Liu, Y.; Lu, H. High-performance conductive double-network hydrogel base on sodium carboxymethyl cellulose for multifunctional wearable sensors. *Carbohydr. Polym.* **2025**, *350*, 122943. [CrossRef] [PubMed]
15. Wan, L.; Li, P.; Yan, M.; Wang, J.; Li, X. Strong, self-healing, shape memory paa-pani/pva/pda/aop conductive hydrogels with interpenetrating network and hydrogen bond interaction. *Eur. Polym. J.* **2023**, *191*, 112034. [CrossRef]
16. Fu, Y.; Chen, A.; Fu, Z.; Zhang, Q.; Deng, W.; Jiang, L.; Hu, X. Oxidized pullulan/carboxymethyl chitosan hydrogel with salidroside for enhanced wound healing. *Int. J. Biol. Macromol.* **2026**, *382*, 154369. [CrossRef] [PubMed]
17. Li, S.; Gao, J.; Xu, L.; Zheng, G.; Kong, Y. A carboxymethyl chitosan-based self-degradable and self-healing hydrogel with photothermal antibacterial and antioxidant properties for wound repair. *Int. J. Biol. Macromol.* **2026**, *353*, 151295. [CrossRef] [PubMed]
18. Ding, F.; Fu, L.; Huang, X.; Shi, J.; Povey, M.; Zou, X. Self-healing carboxymethyl chitosan hydrogel with anthocyanin for monitoring the spoilage of flesh foods. *Food Hydrocoll.* **2025**, *165*, 111270. [CrossRef]
19. Rahmatpour, A.; Emami Kian, M.; Soleimani, P. Natural biopolymer-based injectable, self-healing hydrogel via self-assembly of pectin and quaternized guar gum for targeted treatment of colon cancer. *Biomacromolecules* **2026**, *27*, 5055–5078. [CrossRef] [PubMed]
20. Khan, N.; Kumar Yadav, S.; Saneja, A. Development of electrospun pullulan nanofibers encapsulating naringenin/sulfobutylether-β-cyclodextrin inclusion complex for rapid dissolution and antioxidant activity. *Int. J. Biol. Macromol.* **2025**, *330*, 147961. [CrossRef] [PubMed]
21. Panatdasirisuk, W.; Chantana, W.; Hawan, A.; Wongjeen, P.; Champreda, V. Pectin-encapsulated amorphous naringenin with enhanced aqueous solubility prepared by simple coacervation and precipitation. *Sustain. Food Technol.* **2026**, *4*, 3280–3288. [CrossRef]
22. Chakraborty, S.; Karmakar, V.; Chatterjee, K.; Chatterjee, A.; Dwivedi, M.; Gorain, B. Chitosan nanoparticle-mediated nose-to-brain delivery of naringenin: Attenuating memory decline in experimental animals via behavioural assessment and modulation of biochemical parameters. *Int. J. Biol. Macromol.* **2025**, *286*, 138336. [CrossRef] [PubMed]
23. George, D.; Maheswari, P.U.; Meera, K.M.; Begum, S. Cysteine conjugated chitosan based green nanohybrid hydrogel embedded with zinc oxide nanoparticles towards enhanced therapeutic potential of naringenin. *React. Funct. Polym.* **2020**, *148*, 104480. [CrossRef]
24. Gou, Y.; Wang, A.; Liu, J.; Ding, B.; Song, W.; Sun, Q.; Qu, W.; Zhou, X.; Jiang, L.; Guo, H.; et al. Thermo-responsive mechanically active hydrogel based on dual dynamic covalent cross-linked with antibacterial and antioxidant activity for wound healing. *Chem. Eng. Sci.* **2026**, *323*, 123186. [CrossRef]
25. Shen, Z.; Lin, J.; Lian, X.; Wang, K.; Niu, H. Mechanically robust and highly conductive hydrogels with synergistic cross-linking networks for flexible supercapacitors. *Chem. Eng. J.* **2026**, *544*, 178951. [CrossRef]

26. Shi, S.; Wang, J.; Wang, W.; Chen, H.; Bai, L.; Yang, H.; Yang, L.; Wei, D.; Yin, K. Design of antifreeze, self-healing nanocomposite hydrogels with proline and functional cellulose nanocrystals for the application in wearable flexible sensors. *Eur. Polym. J.* **2024**, *220*, 113452. [CrossRef]
27. Liu, P.; Wei, K.; Liu, Y.; Bai, L.; Chen, H.; Wang, W.; Yang, L.; Yang, H.; Wei, D. Dual antifreeze and sustained release cellulose nanocrystal-humic acid nanocomposite hydrogel for soilless cultivation. *Biomacromolecules* **2026**, *27*, 1724–1735. [CrossRef] [PubMed]
28. Xu, S.; Kong, D.; Qin, F.; Wang, X.; Zhang, M.; Wu, P.; Mo, Z.; Guo, H.; Yu, H. A dynamically cross-linked la/arg/nma hydrogel with integrated self-adhesion, self-healing, and ionic conductivity for flexible wearable sensors and triboelectric nanogenerators. *Nano Energy* **2026**, *155*, 112094. [CrossRef]
29. Zeng, Z.; Xin, Q.; Zhao, T.; Yang, G.; Liang, S.; Lin, J. Strong interfacial adhesion between electrode and hydrogel electrolyte enabled by catechol groups for flexible supercapacitors with anti-freezing and self-healing properties. *Polymer* **2026**, *363*, 130580. [CrossRef]
30. Gao, C.; Zhu, J.; Wu, H.; Chen, J.; Zhu, P.; Gao, Q. A transparent ionic conductive poly (vinyl alcohol)/poly (γ-glutamic acid)/licl hydrogel with long-lasting anti-freezing, water retention, self-adhesion, self-healing and self-regeneration for wearable sensors. *Polymer* **2025**, *328*, 128461. [CrossRef]
31. Song, X.; Guo, J.; Zhang, Y.; Guan, F.; Tao, J.; Yao, Q.; Ji, X. Multi-network hydrogel-based stretchable, self-adhesive, and self-healing self-powered flexible sensors for multi-scale, dynamic and static strain/pressure sensing. *Colloids Surf. A* **2025**, *708*, 136035. [CrossRef]
32. Zhang, X.; Sun, Q.; Yu, X.; Wang, W.; Bai, L.; Chen, H.; Wei, K.; Yang, L. Polydopamine-modified mxene toward anti-freezing and self-healing hydrogel flexible sensors. *Chem. Eng. J.* **2025**, *526*, 171342. [CrossRef]
33. Fang, D.; Bian, J.; Xiang, Y.; Wang, Y.; Zhu, T.; Kang, Y. Self-assembled zwitterionic lignin-induced joint enhancement of mechanics and adhesion in high-performance hydrogels for flexible strain sensors. *Biomacromolecules* **2025**, *26*, 8652–8667. [CrossRef] [PubMed]
34. Liu, P.; Xiao, W.; Bai, L.; Wang, W.; Chen, H.; Yang, L.; Yin, K.; Yang, H.; Wei, D. Surface functionalization of cellulose nanocrystals for fabricating of anti-freezing and self-healing nanocomposites hydrogels. *Eur. Polym. J.* **2024**, *216*, 113269. [CrossRef]
35. He, S.; Fang, H.; Liu, J.; Wu, X.; Liu, Z.; Gu, W.; Shao, W. Fabrication of anti-freezing and self-healing hydrogel sensors based on carboxymethyl guar gum and poly(ionic liquid). *Int. J. Biol. Macromol.* **2024**, *279*, 135112. [CrossRef] [PubMed]
36. Liu, Z.; Liu, J.; He, S.; Wu, X.; Wei, X.; Shao, W. Self-healing and self-adhesion conductive hydrogels reinforced by carboxylated carbon nanotubes for high-performance wearable strain sensors. *ACS Appl. Nano Mater.* **2024**, *7*, 7653–7662. [CrossRef]
37. Simayi, R.; Wang, J.; Sawut, A.; Cheng, L. Preparation of triple-network CS-QCH-TA/PAA hydrogels with enhanced mechanical properties for flexible sensors. *J. Mech. Behav. Biomed. Mater.* **2026**, *176*, 107353. [CrossRef] [PubMed]
38. Tan, S.; Teng, F.; Huang, Y.; Zhang, S.; Li, A. Ultrastretchable and self-healing polyacrylic acid hydrogel strain sensor with pt nanoparticles-modified MXene for machine learning-assisted gesture recognition. *ACS Appl. Nano Mater.* **2026**, *9*, 3334–3345. [CrossRef]
39. Chen, D.; Lin, Y.; Lu, S.; Cheng, C.; Lin, W.; Feng, J.; Li, J.; Yu, M.; Feng, Y.; Wu, Y.; et al. Self-healing hydrogels for flexible underwater motion sensing and rapid information transmission. *Langmuir* **2026**, *42*, 14804–14816. [CrossRef] [PubMed]
40. Cui, Y.; Liu, J.; Zhang, R.; Liu, P. Fabrication of mechanically enhanced self-healing hydrogels based on the synergistic effect of curcumin and CMC-Na for strain-sensing applications. *ACS Appl. Polym. Mater.* **2026**, *8*, 17273–17286. [CrossRef]
41. Liu, C.; Liu, Z.; Lu, B. Self-healing and tough polyacrylic acid-based hydrogels for micro-strain sensors. *Gels* **2025**, *11*, 475. [CrossRef] [PubMed]

Disclaimer/Publisher's Note: The statements, opinions and data contained in all publications are solely those of the individual author(s) and contributor(s) and not of MDPI and/or the editor(s). MDPI and/or the editor(s) disclaim responsibility for any injury to people or property resulting from any ideas, methods, instructions or products referred to in the content.